Available online at www.sciencedirect.com
ScienceDirect
Trans. Nonferrous Met. Soc. China 25(2015) 3578−3584
Transactions of Nonferrous Metals Society of China
www.tnmsc.cn

Deformation behaviors and processing maps of CNTs/Al alloy composite fabricated by flake powder metallurgy

Wei-jun HE[1], Chun-hong LI[1], Bai-feng LUAN[1], Ri-sheng QIU[1], Ke WANG[1], Zhi-qiang LI[2], Qing LIU[1]

1. College of Materials Science and Engineering, Chongqing University, Chongqing 400044, China;
2. State Key Laboratory of Metal Matrix Composites, Shanghai Jiao Tong University, Shanghai 200240, China

Received 11 December 2014; accepted 13 May 2015

Abstract: Deformation behaviors of CNTs/Al alloy composite fabricated by the method of flake powder metallurgy were investigated by hot compression tests, which were performed in the temperature range of 300−550 °C and strain rate range of 0.001− 10 s^{-1} with Gleeble−3500 thermal simulator system. Processing maps of the CNTs/Al alloy at different strains were calculated to study the optimum processing domain. Microstructures before and after hot compressions were characterized by electron backscattered diffraction (EBSD) method. Stress−strain curves indicate that the flow stress increases with the increase of strain rate and the decrease of temperature. The processing maps of the CNTs/Al alloy at different strains show that the optimum processing domain is 500−550 °C, 10 s^{-1} for hot working. EBSD analysis demonstrates that fully dynamic recrystallization occurs in the optimum processing domain (high strainrate 10 s^{-1}), whereas the main soften mechanism is dynamic recovery at low strain rate (0.001 s^{-1}).

Key words: CNTs/Al alloy composite; flake powder metallurgy; recrystallization; processing map; flow stress

1 Introduction

Recently, more and more researches have been carried out on metal matrix composites (MMC) [1,2], which generally combine the good mechanical properties of the metal matrix and the reinforcements. Carbon nanotubes (CNTs) were reported having very high elastic modulus (about 1 TPa) [3] and tensile strength (about 10−100 times that of steel) [4]. Additionally, CNTs can endure 20%−30% deformation before failure [5]. Thus, CNT is considered to be a kind of good material to reinforce metals. In the past years, much attention [6,7] has been paid on the CNTs reinforced composites, for example CNTs/Al [8,9]. These composites generally show much improvement on the mechanical properties, such as yield strength, elastic modulus or wear resistance, compared with the matrix metals. However, compared with matrix aluminum alloys, CNTs reinforced composites are generally more sensitive to process variables due to the presence of hard reinforcements. Hence, it is important to evaluate the workability of the CNTs/Al alloy composites.

A processing map shows the processing space, i.e., the processing conditions for stable and unstable plastic deformations on the axes of temperature and strain rate. Processing map on the basis of dynamic material model (DMM) has been widely used to understand the hot workability of many materials [10−14], especially for some materials which have poor workability. However, few researches have been reported to study the workability of CNTs/Al alloy by processing map. The aim of the current work is to investigate the hot deformation behavior of CNTs/Al alloy composites and to probe its optimized processing parameters by processing map. A series of hot compressions were carried out on a kind of CNTs/Al alloy composite fabricated by flake powder metallurgy [15,16]. The effects of deformation strain and strain rate on the flow behaviors of the CNTs/Al alloy composite were discussed. Then, to study the optimum processing domain, processing maps at different strains were established based on the true stress−strain curves. Microstructure analysis was performed to verify the

Foundation item: Project (2012AA030311) supported by the National High-tech Research and Development Program of China; Project (51421001) supported by the National Natural Science Foundation of China; Project (106112015CDJXY130002) supported by the Fundamental Research Funds for the Central Universities, China

Corresponding author: Bai-feng LUAN; Tel: +86-23-65106067; E-mail: bfluan@cqu.edu.cn

DOI: 10.1016/S1003-6326(15)63997-8

results predicated by the processing map. The presented reasonable process parameters can provide important guideline for the processing techniques of the CNTs/Al alloy composite.

2 Processing map theory

Deformation temperature and strain rate are the most important two factors that affect properties of material subjecting hot deformation. Choosing a set of proper parameters is one of the main challenges for a forming process. Processing maps can provide the basis for the parameter selection. Processing map based on the dynamic material model (DMM) has been widely accepted. According to the DMM, the work-piece is considered as a power dissipater. At any given strain and temperature, the total power P consists of two complementary parts: G represents the power dissipation through plastic deformation, most of which is converted into heat, and J stands for the power dissipation through microstructure transition, such as dynamic recovery, dynamic recrystallization, phase transformations, as well as damage of the material [17]. During plastic flow, P is expressed as follows [18]:

$$P=\sigma\dot{\varepsilon}=G+J=\int_0^{\dot{\varepsilon}}\sigma \mathrm{d}\dot{\varepsilon}+\int_0^{\sigma}\dot{\varepsilon}\mathrm{d}\sigma \tag{1}$$

where σ is the flow stress (MPa) and $\dot{\varepsilon}$ is the strain rate (s^{-1}).

For the given strain and temperature, the flow stress can be represented as

$$\sigma=K\dot{\varepsilon}^m \tag{2}$$

where m is the strain rate sensitivity, K is a material constant. Based on Eq. (1), the variable G and J can be related by the parameter m (the strain rate sensitivity), which is given as follows:

$$\left(\frac{\partial J}{\partial G}\right)_{\varepsilon,T}=\frac{\partial P}{\partial G}\frac{\partial J}{\partial P}=\frac{\sigma}{\dot{\varepsilon}}\frac{\mathrm{d}\dot{\varepsilon}}{\mathrm{d}\sigma}=\left[\frac{\partial \ln\sigma}{\partial \ln\dot{\varepsilon}}\right]_{\varepsilon,T}=m \tag{3}$$

At any deformation temperature and strain, J can be obtained by combining Eqs. (1) and (2) and is expressed by

$$J=\sigma\dot{\varepsilon}-\int_0^{\dot{\varepsilon}}\sigma \mathrm{d}\dot{\varepsilon}=\frac{m}{m+1}\sigma\dot{\varepsilon} \tag{4}$$

For the ideal linear dissipating body, m=1 and $J=J_{\max}=\sigma\dot{\varepsilon}/2=P/2$, and the power dissipation capacity of the material can be evaluated by the efficiency of power dissipation, η, which is defined as follows:

$$\eta=\frac{J}{J_{\max}}=\frac{2m}{m+1} \tag{5}$$

With the change of deformation temperature and strain rate, η varies, which represents the characteristics of power dissipation through microstructure transition.

Considering that the flow stress−strain rate curve may disobey the power law, the following criterion [19] for the occurrence of flow instabilities is used in the present work:

$$2m<\eta \text{ or } m<0 \tag{6}$$

3 Experimental

The CNTs reinforced aluminum alloy composite was fabricated with flake powder metallurgy [16]. There were three steps in the flake powder metallurgy processing [15]. Firstly, nanoflake aluminum alloy powder with chemical composition Al−1%Mg−0.5%Si (mass fraction) was prepared by ball-milling in an attritor at 423 r/min at room temperature for 4 h, followed by surface modification with PVA. Then, mutil-wall CNTs (30−50 nm in diameter, 2−4 μm in length) functionalized with carboxyl groups, were dispersed into water by ultrasonicating and mixed with the as-prepared Al alloy nanoflakes. After mechanical stir, the mix powder was dried in 500 °C Ar atmosphere and compacted under pressure of 50 MPa at 500 °C. Finally, the compacted CNTs/Al alloy composite with 2% CNTs (volume fraction) was extruded at 475 °C with extrusion ratio of 10:1. The microstructure of the prepared composite is shown in Fig. 1, which shows that the extruded multilayer structures can be observed from the vertical section of the extrusion specimens.

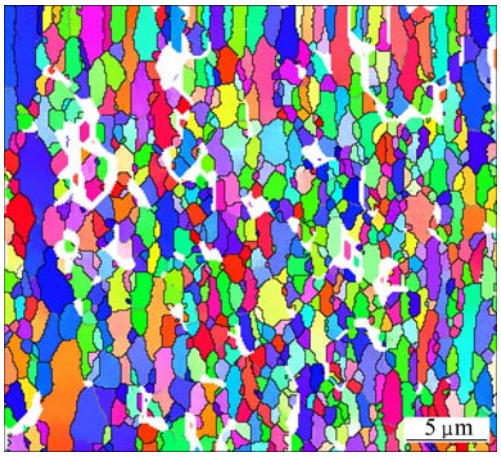

Fig. 1 Initial microstructure of CNTs/Al−Mg−Si composite

For isothermal compression testing, cylindrical specimens with the diameter of 8 mm and height of 12 mm were machined. The specimens were compressed in the temperature range of 300−550 °C (with 25 °C as the increment) and the strain rates 0.001, 0.01, 0.1, 1, 5, and 10 s^{-1} using the Gleeble−3500 thermo- mechanical simulator. In order to reduce the effect of friction, a graphite lubricant was used between the specimens and

the crossheads. All specimens were deformed to the reduction rate of 50% and water-quenched from test temperatures.

The microstructures of the composites before and after hot compression were characterized by field emission scanning electron microscopy (FE-SEM) on a FEI Nova 400 electron microscope.

4 Results and discussion

4.1 Flow stress

Figure 2 displays typical stress−strain curves of the CNTs/Al alloy composite at different temperatures and strain rates. As shown in Fig. 2, the flow stresses of the CNTs/Al alloy composite increase sharply with the increasing strain until peak flow stress, which should be attributed to the increase of dislocation density. These accumulated dislocations could significantly impede further deformation and thus lead to the higher strength (work hardening). For low strain rates (0.001, 0.01 and 0.1 s^{-1}), the flow stresses after the peak stress almost stay constantly. Whereas, after the peak point, the flow stresses start to decrease at high deformation strain rates (5 and 10 s^{-1}).

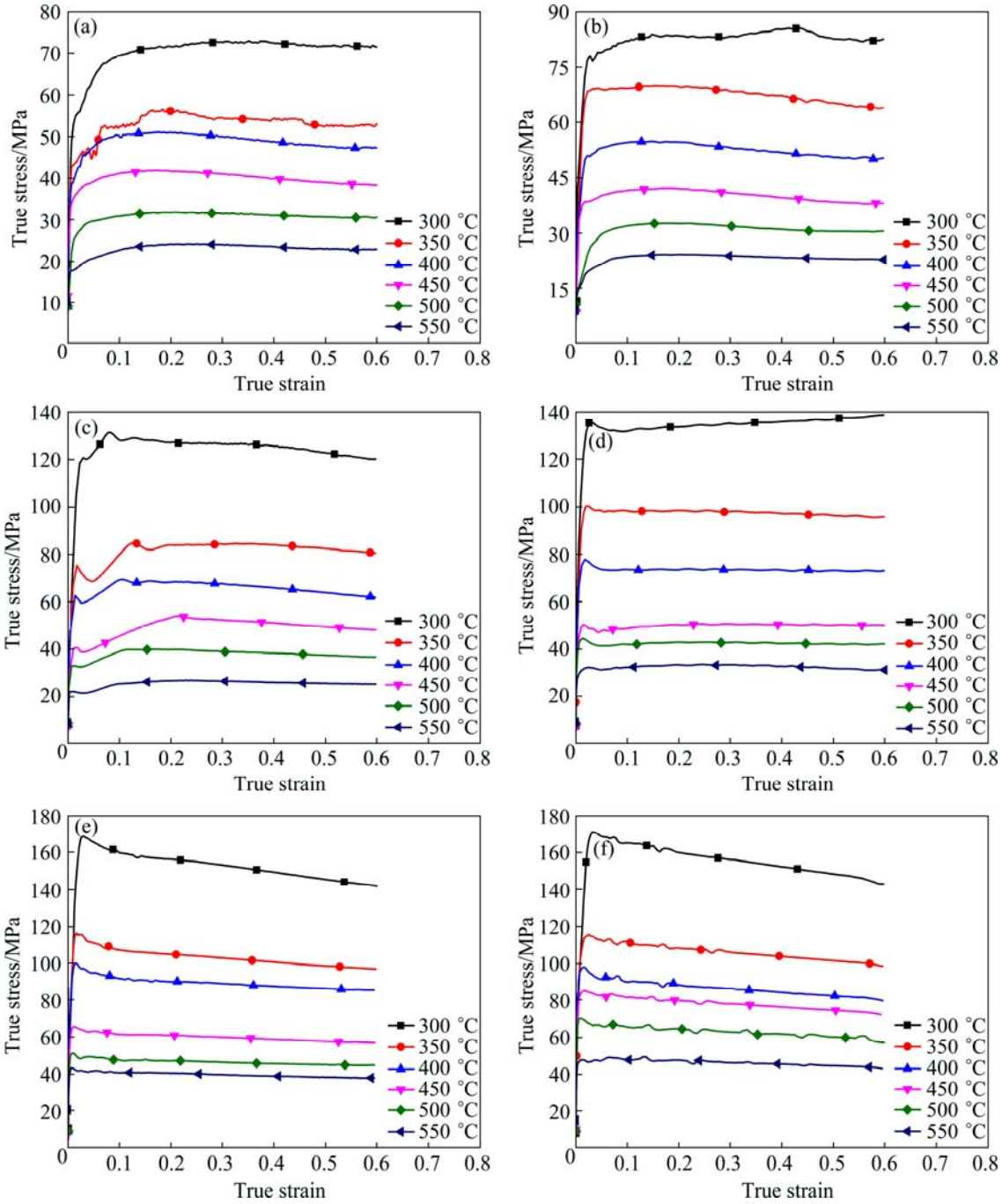

Fig. 2 Typical stress−strain curves for CNTs/Al−Mg−Si composite at various temperatures: (a) 0.001 s^{-1}; (b) 0.01 s^{-1}; (c) 0.1 s^{-1}; (d) 1 s^{-1}; (e) 5 s^{-1}; (f) 10 s^{-1}

The characteristics of these flow stress curves can be explained in terms of work hardening and flow softening phenomenon. Essentially, during hot compression, there is a dynamic competitive procedure between the working hardening caused by dislocation reduplication, pile-up and tangle and the softening caused by the dislocation rearrangement (dynamic recovery) and dynamic recrystallization. For the CNTs/Al−Mg−Si composite, when the strain rate is low, the dynamic recovery and the work hardening achieve a balance at large strain (0.3) as shown in Figs. 2(a)−(c). When the strain rate is high, as demonstrated in Figs. 2(e) and (f), it is the dynamic recrystallization that is competitive with the work hardening. These characteristics may be due to the high stacking fault energy of aluminum alloy, which makes the dynamic recrystallization be only activated at high strain rates.

4.2 Processing maps

A superimposition of the power dissipation map over the instability map gives a processing map, which reveals the deterministic domains where individual microstructure processes occur and the limiting conditions for the regimes of flow instability. By processing under conditions of the highest efficiency in the "safe" domains and avoiding the regimes of flow instabilities, the intrinsic workability of the material may be optimized and microstructure control may be achieved.

Processing maps of CNTs/Al alloy composites at strains of 0.2, 0.3, 0.4 and 0.5 are shown in Fig. 3. The maps obtained at strains of 0.2, 0.3, 0.4 and 0.5 are essentially similar. It indicates that strain does not have significant influence. The maps of CNTs/Al alloy composite display a clear domain in the temperature range of 500−550 °C and strain rate of 10 s^{-1} with peak efficiency of about 30%. To confirm the predication of processing map results, microstructure observations were carried out, as shown in the next section.

4.3 Microstructure analysis

Microstructure of the CNTs/Al alloy composite after hot deformation was characterized with EBSD method. Typical microstructures after deformation at different temperatures and strain rates are shown in Figs. 4 and 5. For each specimen, microstructure was

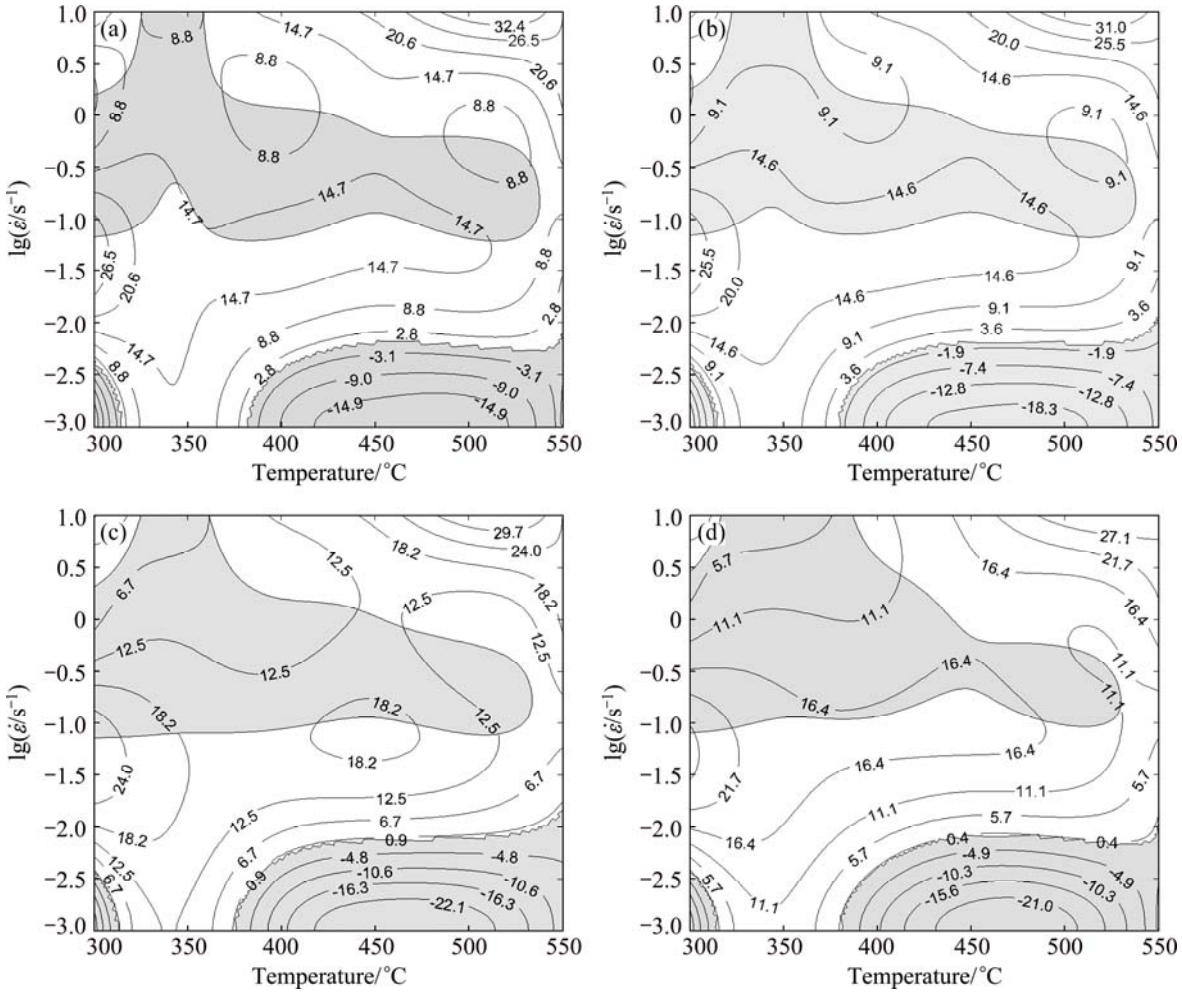

Fig. 3 Processing maps of CNTs/Al−Mg−Si alloy composite at different strains: (a) 0.2; (b) 0.3; (c) 0.4; (d) 0.5

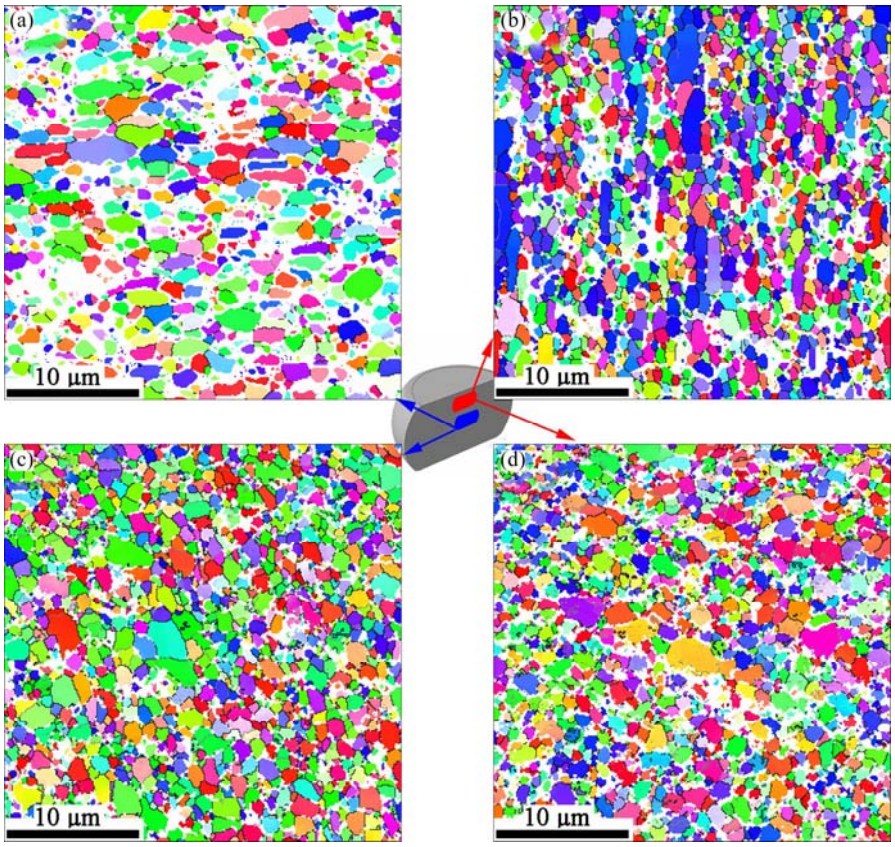

Fig. 4 Microstructures of CNTs/Al alloy composite deformed at 475 °C: (a) 0.001 s^{-1}, center; (b) 0.001 s^{-1}, side; (c) 10 s^{-1}, center; (d) 10 s^{-1}, side

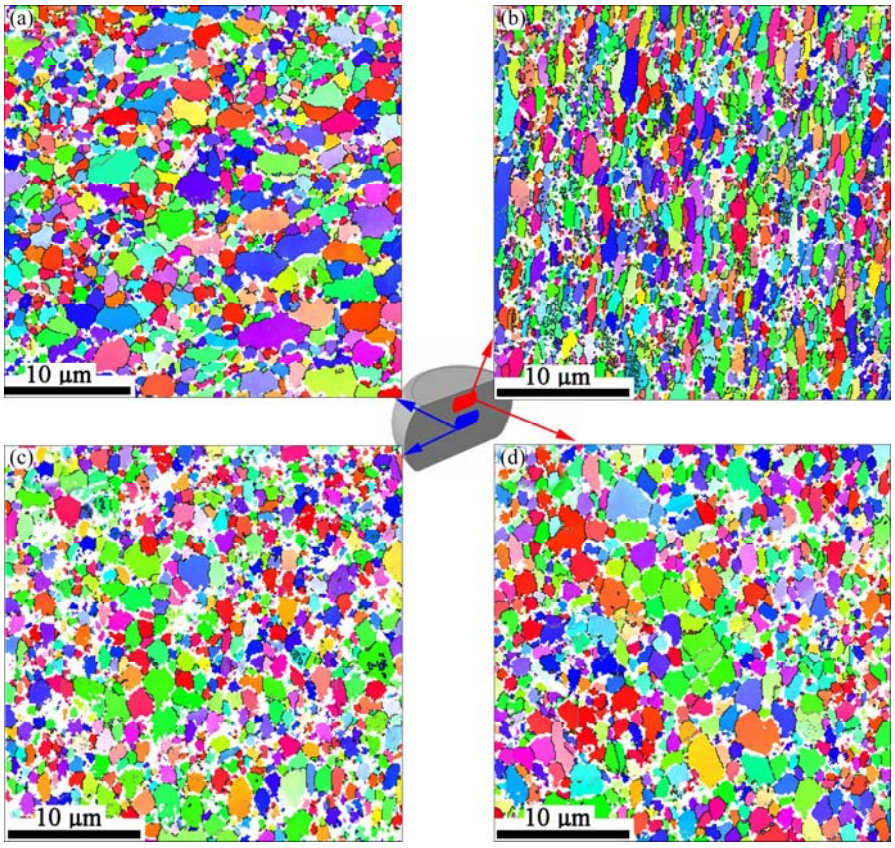

Fig. 5 Microstructures of CNTs/Al alloy composite deformed at 550 °C: (a) 0.001 s^{-1}, center; (b) 0.001 s^{-1}, side; (c) 10 s^{-1}, center; (d) 10 s^{-1}, side

observed at two different regions, center and side regions. The locations for the microstructure observation are schematically presented in Figs. 4 and 5. Generally, due to the friction between specimen and deformation machine, the center region has larger deformation compared with the side region.

After hot compression, Figs. 4 and 5 indicate that the layer structures have been replaced by near equiaxial grains in the center of the specimens no matter what the deformation condition is. For the side region of specimen, it is different. The layer structures are preserved when the strain rate is low (0.001 s^{-1}), as shown in Figs. 4(b) and 5(b). Whereas, when the strain rate is high (10 s^{-1}), it is near equiaxial grain structure. This suggests that full dynamic recrystallization has been achieved at high strain rate, which is considered to be beneficial. At low strain rate, dynamic recrystallization only occurs in part of the specimen and dynamic recovery is assumed to be the main soften mechanism. These microstructures agree well with the results of stress−strain curves provided in Section 4.1.

Compared with the microstructure after deformation at low temperature (475 °C), the microstructures deformed at high temperature (550 °C) are more homogenous in center and side regions, as shown in Figs. 4(c) and (d) and Figs. 5(c) and (d). Therefore, in our research range, high strain rate (10 s^{-1}) and high temperature (550 °C) are beneficial to obtain full dynamic recrystallized and homogenous microstructure. These results confirm the predication of the processing maps, as shown in Fig. 3.

5 Conclusions

1) In the strain rate range from 0.001 to 10.0 s^{-1} and the temperature range from 300 to 550 °C, the flow stress of CNTs/Al alloy composites decreases with the increase of deformation temperature, meanwhile, increases with the increase of strain rate.

2) In the temperature range from 300 to 550 °C, full dynamic recrystallization can be achieved at high strain rate (10.0 s^{-1}), whereas the main soften mechanism is dynamic recovery at low strain rate (0.001 s^{-1}).

3) The processing maps of CNTs/Al alloy composites at strains of 0.2, 0.3, 0.4 and 0.5 exhibit that safe processing domains are in the temperature range of 500−550 °C, 10 s^{-1}, which are confirmed by the microstructure analysis based on EBSD data.

References

[1] XIU Zi-yang, WANG Xu, HUSSAIN M, FENG Chao, JIANG Long-tao. Effect of heat treatment on microstructure and thermophysical properties of diamond/2024 Al composites [J]. Transactions of Nonferrous Metals Society of China, 2013, 23(12): 3584−3591.

[2] WANG Xiao-jun, HU Xiao-shi, NIE Kai-bo, WU Kun, ZHENG Ming-yi. Hot extrusion of SiCp/AZ91 Mg matrix composites [J]. Transactions of Nonferrous Metals Society of China, 2012, 22(8): 1912−1917.

[3] TREACY M M, EBBESEN T W, GIBSON J M. Exceptionally high Youngs modulus observed for individual carbon nanotubes [J]. Nature, 1996, 381: 678−680.

[4] YU M F, FILES B S, AREPALLI S, RUOFF R S. Tensile loading of ropes of single wall carbon nanotubes and their mechanical properties [J]. Physical Review Letters, 2000, 84: 5552−5555.

[5] FALVO M R, CLARY G J, TAYLOR R M, CHI V, BROOKS F P, WASHBRN S, SUPERFINE R. Bending and buckling of carbon nanotubes under large strain [J]. Nature, 1997, 389: 582−584.

[6] AN Z L, TODA M, ONO T. Improved thermal interface property of carbon nanotube–Cu composite based on supercritical fluid deposition [J]. Carbon, 2014, 75: 281−288.

[7] CHEN X H, CHEN C S, XIAO H N, CHENG F Q, ZHANG G, YI G J. Corrosion behavior of carbon nanotubes–Ni composite coating [J]. Surface and Coatings Technology, 2005, 191: 351−356.

[8] JIANG L, FAN G L, LI Z Q, KAI X Z, ZHANG D, CHEN Z X, HUMPHRIES S, HENESS G, YEUNG W Y. An approach to the uniform dispersion of a high volume fraction of carbon nanotubes in aluminum powder [J]. Carbon, 2011, 49: 1965−1971.

[9] HAO Xiao-ning, ZHANG Hai-ping, ZHENG Rui-xiao, ZHANG Yi-tan, AMEYAMA Kei, MA Chao-li. Effect of mechanical alloying time and rotation speed on evolution of CNTs/Al-2024 composite powders [J]. Transactions of Nonferrous Metals Society of China, 2014, 24(7): 2380−2386.

[10] ZHOU H T, LI Q B, ZHAO Z K, LIU Z C, WEN S F, WANG Q D. Hot workability characteristics of magnesium alloy AZ80—A study using processing map [J]. Materials Science and Engineering A, 2010, 527: 2022−2026.

[11] LI A B, HUANG L J, MENG Q Y, GENG L, CUI X P. Hot working of Ti−6Al−3Mo−2Zr−0.3 Si alloy with lamellar $\alpha+\beta$ starting structure using processing map [J]. Materials & Design, 2009, 30: 1625−1631.

[12] LIN Y C, LI L T, XIA Y C, JIANG Y Q. Hot deformation and processing map of a typical Al−Zn−Mg−Cu alloy [J]. Journal of Alloys and Compounds, 2013, 550: 438−445.

[13] SURESH K, RAO K P, PRASAD YVRK, HORT N, KAINER K U. Investigation of hot workability behavior of as-cast Mg−5Sn−2Ca (TX52) magnesium alloy through processing map [J]. Production & Manufacturing Research, 2014, 2: 241−252.

[14] HAO Shi-ming, XIE Jing-pei, WANG Ai-qin, WANG Wen-yan, LI Ji-wen, SUN Hao-liang. Hot deformation behaviors of 35%SiC_p/2024Al metal matrix composites [J]. Transactions of Nonferrous Metals Society of China, 2014, 24(8): 2468−2474.

[15] JIANG L, LI Z Q, FAN G L, CAO L L, ZHANG D. Strong and ductile carbon nanotube/aluminum bulk nanolaminated composites with two-dimensional alignment of carbon nanotubes [J]. Scripta Materialia, 2012, 66: 331−334.

[16] WEI H, LI Z Q, XIONG D B, TAN Z Q, FAN G L, QIN Z, ZHANG D. Towards strong and stiff carbon nanotube-reinforced high-strength aluminum alloy composites through a microlaminated architecture design [J]. Scripta Materialia, 2014, 75: 30−33.

[17] PRASAD Y V, RAO K P. Processing maps and rate controlling mechanisms of hot deformation of electrolytic tough pitch copper in the temperature range 300−950 °C [J]. Materials Science and Engineering A, 2005, 391: 141−150.

[18] PRASAD Y V, GEGEL H L, DORAIVELU S M, MALAS J C, MORGAN J T, LARK K A, BARKER D R. Modeling of dynamic material behavior in hot deformation: Forging of Ti-6242 [J]. Metallurgical Transactions A, 1984, 15: 1883−1892.

[19] NARAYANA MURTY S V S, NAGESWARA RAO B, KASHYAP B P. Identification of flow instabilities in the processing maps of AISI 304 stainless steel [J]. Journal of Materials Processing Technology, 2005, 166: 268−278.

片状粉末冶金碳纳米管增强铝基复合材料的热变形及加工图

何维均[1]，李春红[1]，栾佰峰[1]，邱日盛[1]，王 柯[1]，李志强[2]，刘 庆[1]

1. 重庆大学 材料科学与工程学院，重庆 400044；
2. 上海交通大学 金属基复合材料国家重点实验室，上海 200240

摘 要：采用 Gleeble−3500D 热模拟试验机在 300~550 °C，0.001~10 s^{-1} 条件下开展了 CNTs/Al 复合材料热变形行为研究，并基于真应力−应变曲线计算得到了 CNTs/Al 复合材料在不同应变时的热加工图。利用电子背散射技术分析了变形前后的显微组织。实验结果表明，在设定的温度下，流变应力随着应变速率的增高而增高，而在设定的应变速率下，流变应力随着温度的增高而降低。在高应变速率条件下，可以获得完全再结晶组织。而在低应变速率条件下，只有部分再结晶，主要的软化机制为动态回复。在本研究所采用的实验条件下，CNTs/Al 复合材料的热变形最优加工工艺参数为 500~550 °C，10 s^{-1}。

关键词：CNTs/Al 复合材料；片状粉末冶金；再结晶；加工图；流变应力

(Edited by Yun-bin HE)